Available online at www.sciencedirect.com
ScienceDirect
International Journal of Pharmaceutics 324 (2006) 103–115
INTERNATIONAL JOURNAL OF PHARMACEUTICS
www.elsevier.com/locate/ijpharm

# Novel interpenetrating network chitosan-poly(ethylene oxide-*g*-acrylamide) hydrogel microspheres for the controlled release of capecitabine☆

Sunil A. Agnihotri, Tejraj M. Aminabhavi *

*Drug Delivery Division, Center of Excellence in Polymer Science, Karnatak University, Dharwad 580 003, India*

Received 30 November 2005; received in revised form 3 April 2006; accepted 28 May 2006
Available online 3 June 2006

**Abstract**

This paper describes the synthesis of capecitabine-loaded semi-interpenetrating network hydrogel microspheres of chitosan-poly(ethylene oxide-*g*-acrylamide) by emulsion crosslinking using glutaraldehyde. Poly(ethylene oxide) was grafted with polyacrylamide by free radical polymerization using ceric ammonium nitrate as a redox initiator. Capecitabine, an anticancer drug, was successfully loaded into microspheres by changing experimental variables such as grafting ratio of the graft copolymer, ratio of the graft copolymer to chitosan, amount of crosslinking agent and percentage of drug loading in order to optimize process variables on drug encapsulation efficiency, release rates, size and morphology of the microspheres. A $2^4$ full factorial design was employed to evaluate the combined effect of selected independent variables on percentage of drug release at 5 h (response). Regression models were used for the response and data were compared statistically using the analysis of variance (ANOVA). Grafting, interpenetrating network formation and chemical stability of the capecitabine after encapsulation into microspheres was confirmed by Fourier infrared spectra (FTIR). Differential scanning calorimetry (DSC) and X-ray diffractometry (XRD) studies were made on drug-loaded microspheres to investigate the crystalline nature of drug after encapsulation. Results indicated amorphous dispersion of capecitabine in the polymer matrix. Scanning electron microscope (SEM) confirmed spherical shapes and smooth surface morphology of the microspheres. Mean particle size of the microspheres as measured by the laser light scattering technique ranged between 82 and 168 μm. Capecitabine was successfully encapsulated into semi-IPN microspheres and percentage of encapsulation efficiency varied from 79 to 87. *In vitro* release studies were performed in simulated gastric fluid (pH 1.2) for the initial 2 h, followed by simulated intestinal fluid (pH 7.4) until complete dissolution. The release of capecitabine was continued up to 10 h. Release data were fitted to an empirical relationship to estimate the transport parameters. Dynamic swelling studies were performed in the simulated intestinal fluid and diffusion coefficients were calculated by considering the spherical geometry of the matrices.


*Keywords:* Chitosan; Poly(ethylene oxide); Capecitabine; Microspheres; Controlled release; Grafting; Interpenetrating polymer network; Factorial design

## 1. Introduction

Capecitabine (see Fig. 1) is a pro-drug that is converted to fluorouracil in the body tissues following the oral administration. It is widely used in the treatment of metastatic colorectal cancer and breast cancer, since it is readily absorbed from the gastrointestinal tract. The recommended daily dose is large, i.e., 2.5 g/m$^2$ and it has a short elimination half-life of 0.5–1 h (Judson et al., 1999). The adverse effects associated with capecitabine include bone-marrow depression, cardiotoxicity, diarrhoea, nausea and vomiting, stomatitis, dermatitis, etc. Hence, formulating capecitabine as a controlled release (CR) dosage form would provide greater or longer *in vitro* and *in vivo* antitumor activity, thereby reducing its toxic side effects. In particular, specific advantages of multi-particulate systems such as microspheres, beads, etc., over other conventional dosage forms like tablets and capsules have been discussed earlier (Agnihotri and Aminabhavi, 2004a). However, the main objective of any CR dosage form is to obtain formulations that would allow the drug to remain at the therapeutic limits for longer time. The development of such pharmaceutical forms can be achieved by using specific polymers that are biocompatible. Among many such polymers, hydrogels have been widely used for developing CR devices. Therefore, it would be of interest to choose such

☆ Part of this paper was presented at the 32nd International Symposium on Controlled Release of Bioactive Materials, Miami, FL, USA, June 2005, #741. This paper is CEPS communication # 79.

* Corresponding author. Tel.: +91 836 2215372; fax: +91 836 2771275.
*E-mail address:* aminabhavi@yahoo.com (T.M. Aminabhavi).

0378-5173/$ – see front matter © 2006 Elsevier B.V. All rights reserved.
doi:10.1016/j.ijpharm.2006.05.061

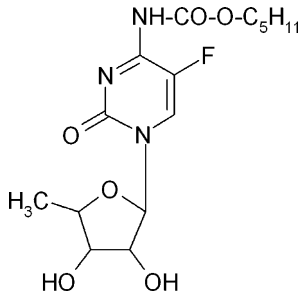


Fig. 1. Chemical structure of capecitabine.

polymers that have appropriate chemical composition, physicochemical nature, biodegradability, chemical stability, mechanical properties, drug release characteristics, desired pharmaceutical dosage form, and administration route (Doelker, 1987).

Hydrogels are the crosslinked hydrophilic polymer networks that are capable of imbibing large amount of water or biological fluids, yet are insoluble in water, but are swollen when immersed. Their water retaining capacity and good biocompatibility makes them important materials in pharmaceutical and biomedical applications. Recently, studies (Ekici and Saraydin, 2004; Verestiuc et al., 2004) on multi-component polymers have been the subject of great interest, since they provide a convenient route to modify the properties in order to meet specific needs of drug delivery. Among these methods, considerable interest has been devoted to the development of interpenetrating polymer network (IPN) hydrogels (Agnihotri and Aminabhavi, 2005; Kurkuri and Aminabhavi, 2004; Kulkarni et al., 2001; Soppimath et al., 2000) for the CR of drugs. IPN is an intimate combination of two polymers both in the same network, which is obtained when at least one polymer is synthesized and/or crosslinked independently in the immediate vicinity of the other (Sperling, 1981). If only one component of the assembly is crosslinked leaving the other in a linear form, the system is termed as semi-IPN. Materials formed from IPNs share the properties that are characteristic of each network (Kosmala et al., 2000). However, homopolymer alone cannot meet the divergent demand in terms of both properties and performance. Therefore, a composite or IPN of two or three different polymers would be a better choice (Changez et al., 2003).

Chitosan [poly(β-(1 → 4)-2-amino-2-deoxy-D-glucose)] is a deacetylated derivative of chitin, which is a naturally occurring polysaccharide, found abundantly in marine crustaceans, insects and fungi (Agnihotri et al., 2004; Ravi Kumar, 2001). Chitosan is a cationic, biocompatible and biodegradable polymer having many biomedical applications. Chitosan has many advantages, particularly in developing micro/nanoparticles. These include: its ability to control the release of active agents, it avoids the use of hazardous organic solvents while fabricating particles, it is soluble in aqueous acidic solution, it is a linear polyamine containing number of free amine groups that are readily available for crosslinking, its cationic nature allows for ionic crosslinking with multivalent anions, it has mucoadhesive character, which increases the residual time at the site of absorption, and so on. Chitosan has been extensively studied as a carrier for many drugs (Agnihotri and Aminabhavi, 2004b; Akbuga and Durmaz, 1994), proteins (Calvo et al., 1997) and gels for the entrapment of cells or antigens (Mi et al., 1999) in pharmaceutical industries. Among the polymers used to design oral CR dosage forms, poly(ethylene oxide) (PEO) has been widely used because of its low toxicity and pH-independent swelling as well as its drug release properties (Apicella et al., 1993; Zhang and McGinity, 1999; Razaghi and Schwartz, 2002). It is a biologically inert, flexible polymer and it helps to improve the mechanical properties of blends when combined with another polymer. In addition, it possesses mucoadhesive character and is nonionic, so that it is compatible with an ion-rich environment. Polyacrylamide is another widely studied hydrogel that possesses soft tissue biocompatibility and an open porous structure that allows the transport of incorporated molecules (Risbud and Bhonde, 2000). It swells in water and retains a significant fraction of water within its structure and possesses achievable degree of control on the physical and chemical behaviors. These desirable features make polyacrylamide a suitable candidate for drug delivery applications.

The present study is aimed at developing novel type of semi-IPN microspheres of chitosan with poly(ethylene oxide-*g*-acrylamide) for the CR of capecitabine. Formulation and process variables affecting the preparation of semi-IPN microspheres and *in vitro* drug release characteristics have been investigated. In this investigation, a $2^4$ full factorial design model was used to investigate the combined influence of four variables: grafting ratio of the graft copolymer (A), ratio of the graft copolymer to chitosan (B), amount of crosslinking agent (C) and percentage of drug loading (D) on percentage of drug release at 5 h. A statistical model with significant interaction terms is derived to predict the percentage of drug release at 5 h. Graft copolymer of PEO and polyacrylamide was prepared in two different grafting ratios. Semi-IPN microspheres were prepared by crosslinking chitosan in the immediate vicinity of the graft copolymer by using glutaraldehyde (GA). Semi-IPN microspheres have been characterized by Fourier transform infrared (FTIR) spectroscopy, differential scanning calorimetry (DSC), X-ray diffraction (XRD), and scanning electron microscope (SEM). Potential applications of the novel semi-IPN matrices for the CR of an anticancer agent, capecitabine, have been investigated.

## 2. Materials and methods

### 2.1. Materials

PEO ($M_w \cong 900{,}000$ g/mol) and CS (medium molecular weight with 75–85% deacetylation), having the viscosity (Brookfield, 1% solution in 1% acetic acid) of 200–800 cps were purchased from Aldrich Chemical Company, Milwaukee, WI, USA. Capecitabine was kindly gifted by Sun Pharmaceutical Ltd., Vadodara, India. Analytical reagent grade samples of acrylamide, ceric ammonium nitrate, GA (25%, v/v), light liquid paraffin, Span® 80, *n*-hexane, acetone and methanol were purchased from S.D. Fine-Chemicals, Mumbai, India. Double distilled water was used throughout the work. All other chemicals were used without further purification.

Table 1
Synthetic details and grafting parameters of PEO-*g*-pAAm copolymers

| Graft copolymer code | Mass of PEO (g) | Mass of AAm (g) | Mass of initiator (g/g of polymer) | Grafting (%) | Grafting efficiency (%) | Conversion of AAm (%) |
|---|---|---|---|---|---|---|
| PEO-1 | 1 | 5 | 0.3 | 408 | 84.7 | 81.6 |
| PEO-2 | 1 | 10 | 0.3 | 850 | 86.4 | 85.0 |

### 2.2. Methods

#### 2.2.1. Synthesis of PEO-grafted-polyacrylamide

PEO-*grafted*-polyacrylamide (PEO-*g*-pAAm) copolymer was prepared by free radical polymerization using ceric ammonium nitrate (CAN) as a redox initiator. Briefly, 1% aqueous solution of PEO was prepared by dispersing the polymer in double distilled water, allowed to hydrate and dissolved overnight under constant stirring in a 250 mL round-bottom flask. To this, a solution of 0.07 or 0.14 mol of acrylamide (AAm) was added and stirred for 1 h at 60 °C. The initiator solution containing $5.47 \times 10^{-4}$ mol of CAN was added to the above mixture. The choice of CAN concentration was based on the preliminary investigation performed with varying concentration of CAN. The CAN concentration of $5.47 \times 10^{-4}$ mol was found to be optimum to complete the grafting reaction. Polymerization was carried out under continuous purging of nitrogen gas with a constant stirring at 60 °C for 5 h. The reaction mixture was cooled and a pinch of quinhydrone was added to quench the reaction. The mass obtained was precipitated in sufficient amount of acetone and the precipitate was washed with methanol:water (8:2) mixture to remove the homopolymer formed. It was assumed that there was no residual acrylamide when quinhydrone was added, i.e., all acrylamide had been incorporated either in the homopolymer or in the grafted PEO. The graft copolymer formed was dried under vacuum (60 mmHg) at 40 °C overnight. The synthetic details are given in Table 1 and reaction scheme is presented in Fig. 2.

Grafting parameters such as percentage of grafting, percentage of grafting efficiency and percentage of conversion of AAm were calculated as:

$$\text{Percentage of grafting} = \left(\frac{\text{Mass of acrylamide in the grafted polymer}}{\text{Mass of polymer taken}}\right) \times 100 \quad (1)$$

$$\text{Percentage of grafting efficiency} = \left(\frac{\text{Mass of grafted polymer}}{\text{Mass of (polymer + acrylamide)}}\right) \times 100 \quad (2)$$

$$\text{Percentage of conversion} = \left(\frac{\text{Mass of acrylamide in the grafted polymer}}{\text{Mass of acrylamide taken}}\right) \times 100 \quad (3)$$

#### 2.2.2. Preparation of microspheres

Chitosan and PEO-*g*-pAAm semi-IPN microspheres containing capecitabine were prepared by emulsion crosslinking. Chitosan and PEO-*g*-pAAm (total polymer concentration of 2%, w/v) were dissolved in 2% aqueous acetic acid solution and stirred overnight to get uniform bubble free solution. Capecitabine equivalent to 25 or 50% (w/w) of dry weight of the polymer was added to the above polymer solution and stirred until a homogenous solution was formed. This solution was emulsified into light liquid paraffin in the presence of 0.5% Span® 80 using Eurostar stirrer (IKA Labortechnik, Germany) at 400 rpm for 10 min. Then, a mixture of different quantities of GA and 1 mL of 5N HCl was added slowly and stirring was continued for 2 h. The hardened microspheres were separated by filtration and washed with *n*-hexane. The microspheres were dried at 50 °C for 24 h and stored in a desiccator until further use. The formation of semi-IPN structure is schematically shown in Fig. 3.

#### 2.2.3. Factorial design

Traditionally, pharmaceutical formulations have been developed by changing one variable at a time. The method is time-consuming and requires lot of imaginative efforts. Moreover, it may be difficult to evolve an ideal formulation using this classical technique, since the combined effects of independent variables are not considered. It is therefore, essential to understand the complexity of the pharmaceutical formulations by using the established statistical tools such as factorial designs. The number of experiments required for these studies depends upon the number of independent variables selected. The factorial design experiments were performed in random order and various formulations of the microspheres were developed. The response was measured as percentage of drug release at 5 h from

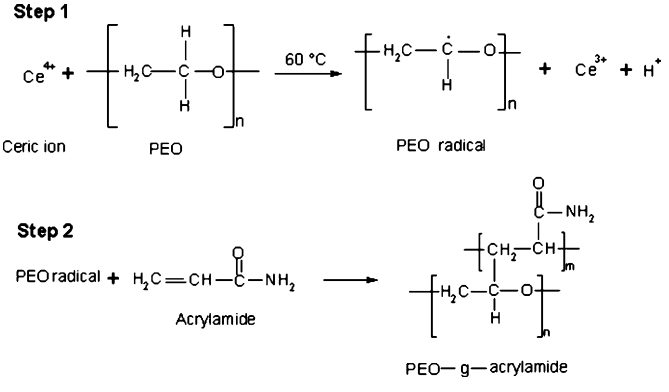


Fig. 2. Reaction scheme to prepare PEO-*g*-pAAm copolymer.

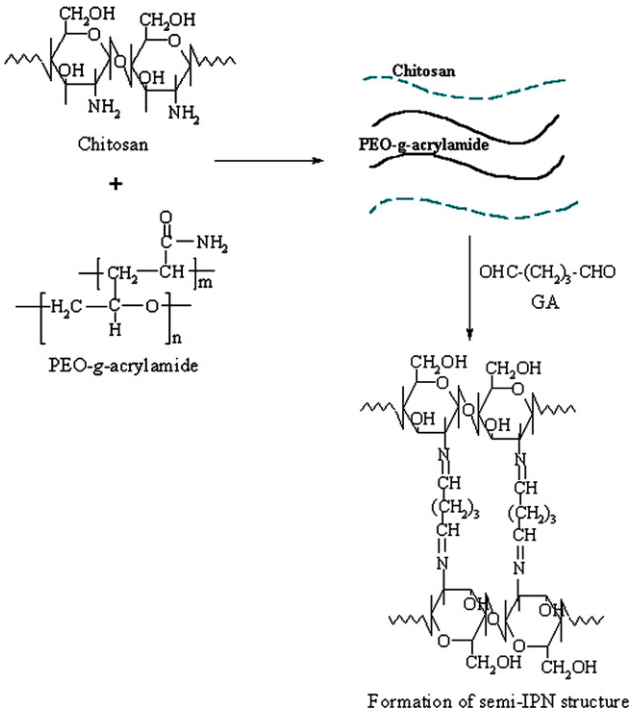


Fig. 3. Schematic representation of the formation of IPN structure.

the microspheres. The design matrix and data obtained from a single replicate of $2^4$ experiments along with the formulation codes are given in Table 2. Microsoft Excel® was used to perform the multiple linear regression analysis. To perform the statistical analyses of the data, the Statistica® software was employed.

### 2.2.4. Capecitabine content

Estimation of drug content was done as per the method adopted earlier (Agnihotri and Aminabhavi, 2004b). Microspheres of known weights were soaked in 50 mL of water for 30 min and sonicated using a probe sonicator (UP 400s, dr. hielscher, GmbH, Germany) for 15 min to break the microspheres and facilitate extraction of the drug. The whole solution was centrifuged using a tabletop centrifuge (Jouan, MR 23i, France) to remove the polymeric debris and polymeric debris was washed twice with fresh solvent (water) to extract any adhered drug. The clear supernatant solution was analyzed for capecitabine content by UV spectrophotometer (Secomam, Anthelie, France) at $\lambda_{max}$ value of 240 nm. The complete extraction of drug was confirmed by repeating the extraction process on the already extracted polymeric debris. The percentage of encapsulation efficiency of the semi-IPN matrix was calculated as reported before (Agnihotri and Aminabhavi, 2004b) and these data for various formulations are presented in Table 3.

### 2.2.5. Particle size measurements

Particle size was measured by using a laser light scattering technique (Mastersizer 2000, Malvern, UK). Size of the microspheres of different formulations was measured by using a dry sample adapter. Completely dried microspheres were placed on the sample tray in an inbuilt vacuum and compressed air system was used to suspend the particles. The laser obscuration range was maintained between 1 and 2%. The volume-mean diameter ($V_d$) was recorded. The analysis was performed in triplicate and average values were used.

### 2.2.6. Swelling studies

To understand the molecular transport of liquids into semi-IPN microspheres, dynamic swelling studies were performed in simulated intestinal fluid (SIF) (without enzymes) by mass measurements. It was found from our preliminary observations that when swelling experiments were performed in simulated gastric fluid (SGF), no significant changes ($P < 0.05$) were observed. Hence, we have studied the swelling of microspheres in SIF. The microspheres were soaked in SIF media maintained at 37 °C. At

Table 2
A design matrix and results of the $2^4$ full factorial experiment

| Formulation code | Independent variables | | | | Independent variables | | | | Run label | Response |
|---|---|---|---|---|---|---|---|---|---|---|
| | A | B | C | D | Grafting ratio | Ratio of graft coplymer:CS | GA (mL) | Drug loading (%) | | Drug release (%) at 5 h |
| F1 | − | − | − | − | 1:5 | 25:75 | 5 | 25 | (1) | 69.23 |
| F2 | − | − | − | + | 1:5 | 25:75 | 5 | 50 | d | 74.15 |
| F3 | − | − | + | − | 1:5 | 25:75 | 10 | 25 | c | 62.22 |
| F4 | − | + | − | − | 1:5 | 50:50 | 5 | 25 | b | 64.51 |
| F5 | + | − | − | − | 1:10 | 25:75 | 5 | 25 | a | 65.62 |
| F6 | − | − | + | + | 1:5 | 25:75 | 10 | 50 | cd | 65.11 |
| F7 | − | + | − | + | 1:5 | 50:50 | 5 | 50 | bd | 66.13 |
| F8 | + | − | − | + | 1:10 | 25:75 | 5 | 50 | ad | 69.14 |
| F9 | − | + | + | − | 1:5 | 50:50 | 10 | 25 | bc | 55.56 |
| F10 | + | − | + | − | 1:10 | 25:75 | 10 | 25 | ac | 57.19 |
| F11 | + | + | − | − | 1:10 | 50:50 | 5 | 25 | ab | 59.03 |
| F12 | − | + | + | + | 1:5 | 50:50 | 10 | 50 | bcd | 60.09 |
| F13 | + | − | + | + | 1:10 | 25:75 | 10 | 50 | acd | 61.03 |
| F14 | + | + | − | + | 1:10 | 50:50 | 5 | 50 | abd | 61.69 |
| F15 | + | + | + | − | 1:10 | 50:50 | 10 | 25 | abc | 51.10 |
| F16 | + | + | + | + | 1:10 | 50:50 | 10 | 50 | abcd | 56.42 |

− and + sign indicates low and high levels of a factor, respectively.

Table 3
Results of percentage of encapsulation efficiency, particle size, molar mass between crosslinks ($M_c$) calculated from Eq. (8), crosslink density ($d_x$) calculated from Eq. (11), parameters, $k$ and $n$, correlation coefficient ($r$) calculated from Eq. (12) and diffusion coefficients ($D$) calculated from Eq. (7)

| Formulation code | Encapsulation efficiency (%) | Volume mean particle size (μm) | $M_c$ (g/mol) | $d_x$ ($10^4$ mol/cm$^3$) | $k$ | $n$ | $r$[a] | $D$ ($10^6$ cm$^2$/s) |
|---|---|---|---|---|---|---|---|---|
| F1 | 84.00 | 142 | 5682 | 5.46 | 0.051 | 0.72 | 0.998 | 7.4 |
| F2 | 86.52 | 139 | 6758 | 3.21 | 0.062 | 0.69 | 0.999 | 9.1 |
| F3 | 83.89 | 82 | 4145 | 8.65 | 0.033 | 0.86 | 0.999 | 4.9 |
| F4 | 84.70 | 165 | 4561 | 7.74 | 0.035 | 0.84 | 0.989 | 5.6 |
| F5 | 82.81 | 150 | 4768 | 7.29 | 0.037 | 0.82 | 0.999 | 6.0 |
| F6 | 85.33 | 88 | 4784 | 7.28 | 0.036 | 0.82 | 0.998 | 6.0 |
| F7 | 86.53 | 167 | 5011 | 6.83 | 0.035 | 0.82 | 0.999 | 6.3 |
| F8 | 87.20 | 154 | 5664 | 5.48 | 0.051 | 0.73 | 0.998 | 7.4 |
| F9 | 78.92 | 93 | 2586 | 11.36 | 0.030 | 0.91 | 0.996 | 2.5 |
| F10 | 79.87 | 89 | 3045 | 10.45 | 0.032 | 0.88 | 0.993 | 3.2 |
| F11 | 80.25 | 168 | 3460 | 10.02 | 0.033 | 0.88 | 0.995 | 3.9 |
| F12 | 82.06 | 96 | 3683 | 9.55 | 0.032 | 0.87 | 0.998 | 4.2 |
| F13 | 83.14 | 88 | 3921 | 9.07 | 0.034 | 0.87 | 0.999 | 4.6 |
| F14 | 84.64 | 159 | 3905 | 9.09 | 0.033 | 0.87 | 0.988 | 4.6 |
| F15 | 81.21 | 95 | 1682 | 13.16 | 0.018 | 0.97 | 0.994 | 1.1 |
| F16 | 85.53 | 98 | 2815 | 10.89 | 0.031 | 0.90 | 0.996 | 2.8 |

[a] The correlation coefficient for the estimation of $k$ and $n$ values.

different time intervals, few microspheres representative of the batch were taken out and blotted off carefully in between tissue papers (without pressing hard) to remove the surface-adhered liquid droplets. The swollen microspheres were then weighed ($w_1$) on an electronic microbalance (Mettler, AE 240, Switzerland) to an accuracy of ±0.01 mg. Microspheres were then dried until attainment of constant mass ($w_2$) in an oven maintained at 60 °C. Usually, the drying process lasted for 5 h. These studies were performed in triplicate for each set of the formulated samples and average values were considered for data analysis. The percentage of equilibrium water uptake was calculated as:

$$\text{Percentage of water uptake} = \left(\frac{\text{Mass of swollen beads } (w_1) - \text{Mass of dry beads } (w_2)}{\text{Mass of dry beads } (w_2)}\right) \times 100 \quad (4)$$

The standard deviation in water uptake data was within 3.0%.

### 2.2.7. In vitro release studies

Even though swelling studies indicated no significant differences ($P < 0.05$) in the swelling behavior in both SGF and SIF media, the *in vitro* study was designed to simulate the GIT conditions when the formulation is administered orally. *In vitro* drug release from different formulations of semi-IPN matrices was investigated in SGF (0.1N HCl, pH 1.2, ionic strength 0.1) for the first 2 h, followed by the SIF [pH 7.4 phosphate buffer (0.05 M potassium dihydrogen phosphate), ionic strength 0.09] (without enzymes) until complete dissolution. These experiments were performed using a fully automated dissolution tester coupled with the UV system (Logan Instruments Corp., Model D 800, NJ, USA) equipped with six baskets at the stirring speed of 100 rpm. A weighed quantity of each sample was placed in 500 mL of dissolution medium maintained at 37 °C. The instrument automatically measures the concentration of drug released at the particular time interval by UV spectrophotometer coupled with flow through cells attached to the instrument and then replaces the solution back into the dissolution bowl. The capecitabine concentration was determined spectrophotometrically at the $\lambda_{max}$ value of 240 nm. These studies were performed in triplicate for each sample and average values were used while data analysis.

### 2.2.8. Fourier transform infrared (FTIR) spectral studies

FTIR spectra of the pristine PEO, pristine acrylamide, PEO-*g*-pAAm, pristine chitosan, placebo microspheres, pristine capecitabine and capecitabine-loaded microspheres were obtained. In order to investigate the possible reaction between GA and capecitabine, pristine capecitabine was treated with GA. The ratio (mL/mg) and concentration of GA as well as capecitabine was kept identical to that used in formulations. The time of exposure was also kept identical to that of microsphere preparation, i.e., 2 h. Then, capecitabine was washed with double distilled water. After drying, FTIR spectrum was recorded. The samples were crushed with KBr to get pellets by applying a pressure of 600 kg/cm$^2$. Spectral scans were taken in the range between 4000 and 500 cm$^{-1}$ on a Nicolet (Model Impact 410, Milwaukee, WI, USA) instrument.

### 2.2.9. Differential scanning calorimetry (DSC) studies

Differential scanning calorimetry (DSC) was performed on pristine capecitabine, placebo microspheres and capecitabine-loaded microspheres. DSC measurements were done on a Rheometric Scientific (DSC-SP, Surrey, UK) by heating the samples from ambient to 400 °C at the heating rate of 10 °C/min in a nitrogen atmosphere (flow rate, 20 mL/min).

### 2.2.10. X-ray diffraction (XRD) studies

The crystallinity of pristine capecitabine and capecitabine-loaded microspheres were evaluated by XRD measurements recorded for pristine capecitabine, placebo microspheres and

drug-loaded microspheres using X-ray diffractometer (x-Pert, Philips, UK). Scanning was done up to $2\theta$ of 50°.

*2.2.11. Scanning electron microscopic (SEM) studies*

SEM images were taken on drug-loaded semi-IPN microspheres. Microspheres were sputtered with gold to make them conducting and placed on a copper stub. Scanning was done using Leica 400, Cambridge, UK instrument at National Chemical Laboratory (NCL), Pune, India (courtesy of Dr. S.B. Halligudi, Catalysis Division, NCL, Pune). Thickness of the gold layer done by gold sputtering was about 15 nm.

## 3. Results and discussion

### *3.1. Synthesis of PEO-grafted-polyacrylamide*

Graft copolymerization of PEO with AAm was achieved by CAN-catalyzed free radical polymerization as presented in Fig. 2. In the first step, hydrogen abstraction from PEO chain takes place and free radical sites are generated on PEO chain. This facilitates the reaction site for AAm monomer on PEO backbone. Two monomer concentrations of 0.07 and 0.14 mol were used, which resulted in percentage of grafting efficiency of 84.7 and 86.4, respectively (see Table 1). The monomer conversion up to 85% was achieved.

### *3.2. Preparation and characterization of microspheres*

Capecitabine-loaded semi-IPN microspheres of CS and PEO-*g*-AAm were prepared by emulsion crosslinking using GA as a crosslinking agent. By this method, percentage of encapsulation efficiency was found to be in the range of 78.9–87.2. The microspheres produced were all spherical with smooth surfaces as revealed by SEM images shown in Fig. 4. Size and size distribution of microspheres were recorded by laser light diffraction technique (Mastersizer-2000, Malvern, UK). Fig. 5 displays the particle size distribution pattern. On a population basis, particle size distribution was found to be unimodal with narrow size distributions. Calculated values of volume-mean particle size of the microspheres are included in Table 3. These data showed a systematic dependence on the amount of crosslinking agent and also on the ratio of graft copolymer to CS used while formulating the microspheres. With an increase in crosslinking agent (for formulations F3, F6, F9, F10, F12, F13, F15 and F16 as compared to formulations F1, F2, F4, F5, F7, F8, F11 and F14, respectively), microspheres having smaller sizes were produced, probably due to the formation of a more rigid network. Also, by increasing the ratio of graft copolymer in the microspheres (for formulations F4, F7, F9, F11, F12, F14, F15 and F16 as compared to formulations F1, F2, F3, F5, F6, F8, F10 and F13, respectively), an increase in the size of microspheres was observed, which could be attributed to the formation of bigger droplets due to increase in the viscosity of solution with increasing concentration of graft copolymer during emulsification. This was evident from our preliminary studies on viscosity of chitosan and PEO-*g*-pAAm, which showed that flow time of PEO-*g*-pAAm solution was higher when compared to that of chitosan solution at the same concentration of both the polymers.

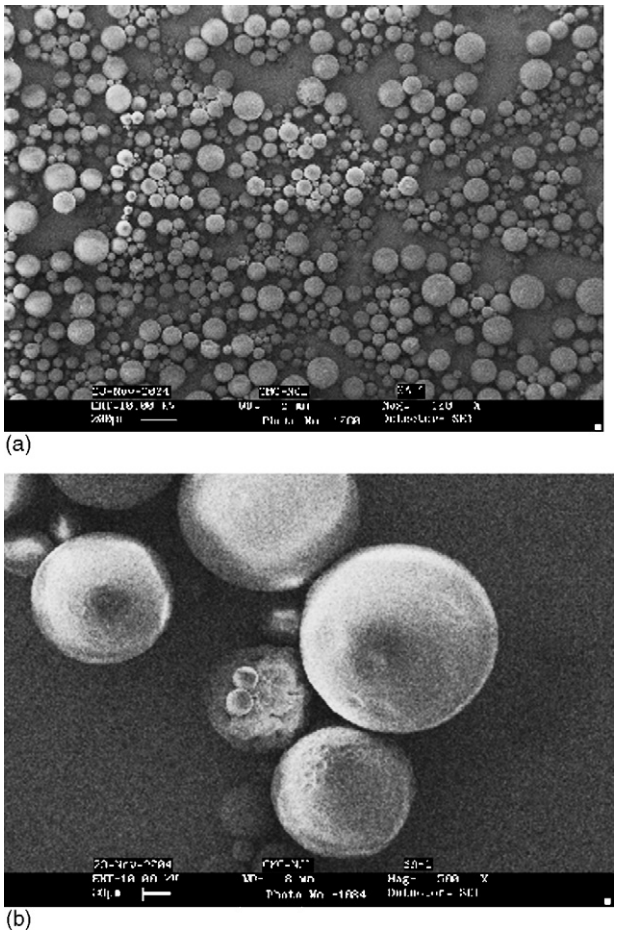
(a)

(b)

Fig. 4. SEM images of the microspheres (formulation F2): (a) group of particles and (b) single particle.

### *3.3. Factorial design*

Effects of individual variables (A, B, C and D) and their interactions between the four variables in the factorial design of experiments was calculated using the table of plus and minus signs for the contrast constants for $2^4$ design as proposed by

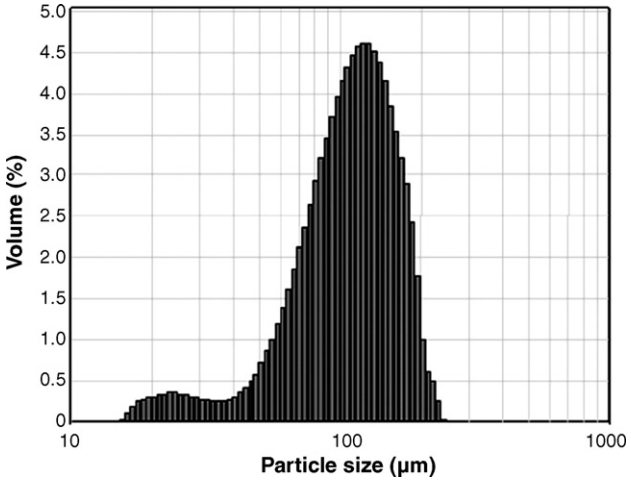


Fig. 5. Particle size distribution of microspheres (formulation F2).

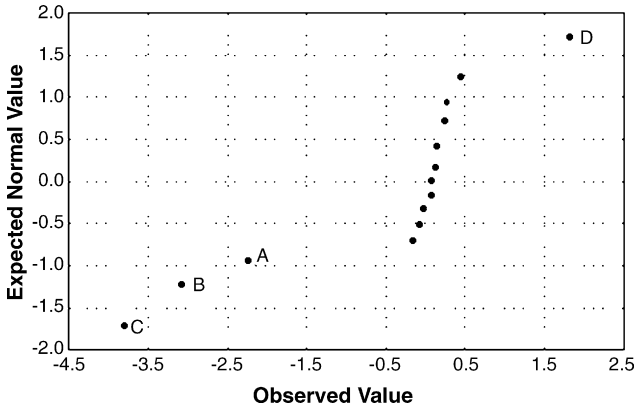


Fig. 6. Normal probability plot of the effects for the $2^4$ factorial design.

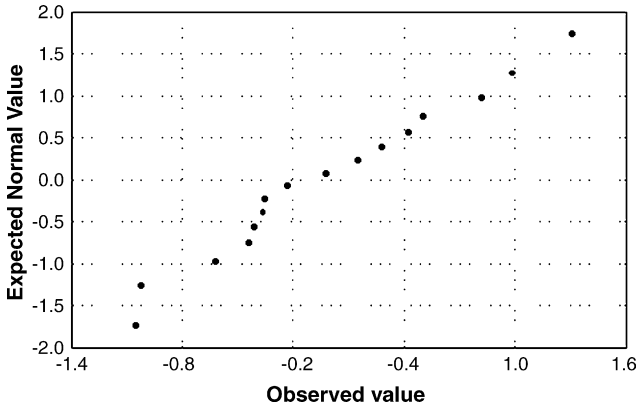


Fig. 7. Normal probability plot of the residuals for the $2^4$ factorial design.

Montgomery (1997). After performing the regression analysis from these contrasts, we have estimated the 15 factorial effects. Since the total number of treatment combinations is large, it is essential to identify factors having significant effects. As suggested by Daniel (1987), a normal probability plot of the estimates of the effects was constructed, which is displayed in Fig. 6. The effects that are normally distributed, with mean zero and variance $\sigma^2$ will tend to fall along a straight line on this plot, whereas significant effects will have nonzero means, and these will not lie along the straight line. Thus, the preliminary model can be specified to contain those effects that are apparently nonzero based on the normal probability plot. The apparently negligible effects are combined as an estimate of error. As seen from the normal probability plot (Fig. 6), important effects that influence the percentage of drug release at 5 h (response) seem to be the main effects of A, B, C and D, which are far from straight line trends. All other effects (interactions), which lie along the straight line, do not significantly influence the percentage of drug release at 5 h.

The correlation between effective experimental variables (A, B, C and D) and the dependant variable (percentage of drug release at 5 h) was calculated by the multiple linear regressions. The method of least squares was used to estimate regression coefficients and the following polynomial equation was derived:

$$Y = 62.389 - 2.236X_1 - 3.073X_2 - 3.799X_3 + 1.831X_4 \quad (5)$$

Here, the coded variables $X_1$, $X_2$, $X_3$ and $X_4$ represent the variables A, B, C and D, respectively. The results comparing the experimentally obtained and model-predicted values of the response are calculated. The predicted values demonstrate a good agreement with the experimental data ($R^2 = 0.986$). A normal probability plot of the residuals is presented in Fig. 7. The points on this plot lie reasonably close to straight line, giving support to our conclusion that A, B, C and D are the only significant effects in this study.

### 3.4. FTIR spectral studies

The grafting of AAm onto PEO was confirmed by FTIR. Fig. 8 compares FTIR spectra of: (a) PEO, (b) AAm and (c) PEO-*g*-AAm. In case of PEO, characteristic bands at 2888 and 1464 $cm^{-1}$ indicate the $–CH_2–$ stretching and bending vibrations, respectively. The band at 1412 $cm^{-1}$ indicates the C–H bending vibrations, while the band at 1097 $cm^{-1}$ confirms the presence of ethereal C–O stretchings. In case of AAm, bands at 1673 and 1610 $cm^{-1}$ indicate amide carbonyl stretching (amide I band) and amide N–H bending (amide II band) vibrations, respectively. The bands at 2925 and 1425 $cm^{-1}$ indicate CH stretching and bending vibrations, respectively. The bands at 3356 and 3185 $cm^{-1}$ are due to primary amide stretching vibrations. The spectra of PEO-*g*-AAm shows bands at 2919 and

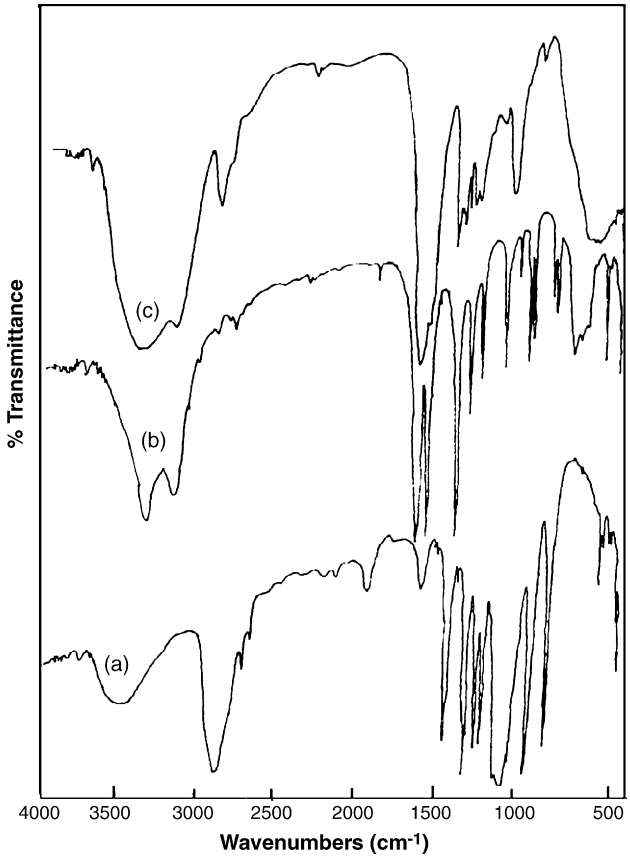


Fig. 8. FTIR spectra of: (a) PEO, (b) AAm and (c) PEO-*g*-pAAm (grafting ratio 1:5).

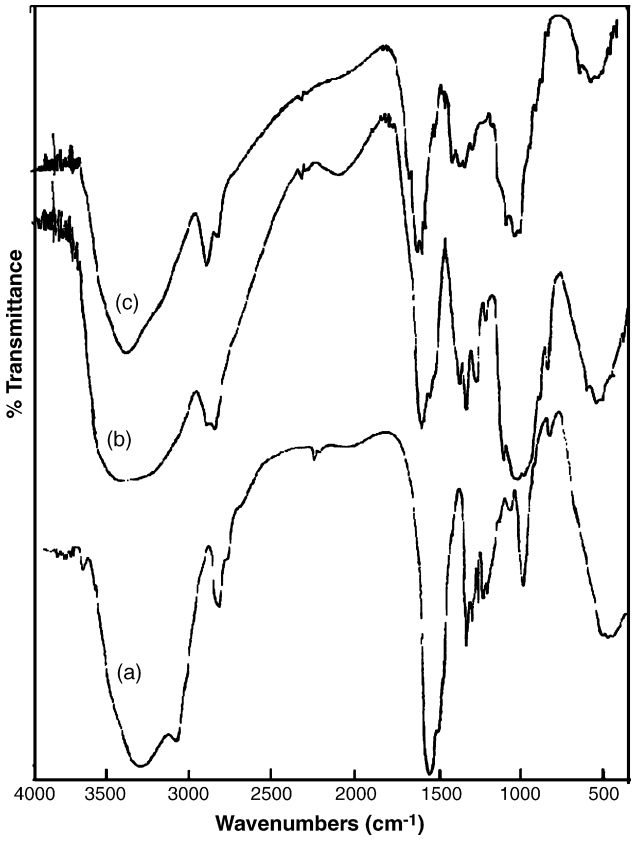


Fig. 9. FTIR spectra of: (a) PEO-*g*-pAAm (grafting ratio 1:5), (b) chitosan and (c) placebo microspheres of formulation F2.

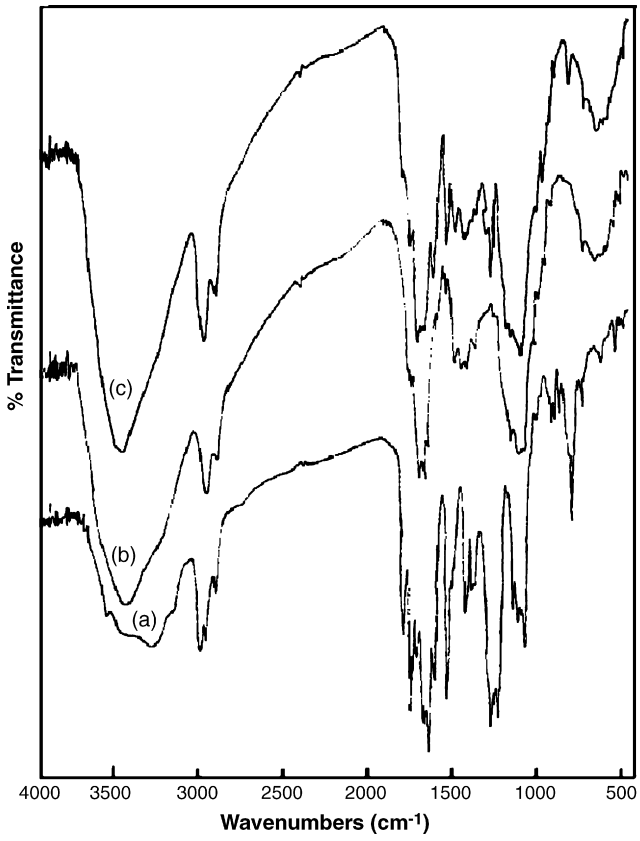


Fig. 10. FTIR spectra of: (a) pristine capecitabine, (b) placebo microspheres of formulation F2 and (c) capecitabine-loaded microspheres (formulation F2).

1455 $cm^{-1}$ due to $–CH_2–$ stretching and bending vibrations, respectively. The band at 1122 $cm^{-1}$ indicate C–O stretching vibrations due to ether group, while those at 1604 and 1665 $cm^{-1}$ indicate amide N–H bending and amide carbonyl stretching vibrations, respectively. It is clear from the FTIR spectrum that the graft copolymer, PEO-*g*-AAm, has both characteristic peaks of PEO and AAm, which could be an effective evidence of grafting.

FTIR was also used to confirm the crosslinking of semi-IPN matrix. Fig. 9 compares the FTIR spectra of: (a) PEO-*g*-AAm, (b) chitosan and (c) placebo microspheres. In case of chitosan, a broad band at 3425 $cm^{-1}$ is attributed to O–H stretching vibrations of the hydroxyl groups. The characteristic band at 1653 $cm^{-1}$ indicates N–H bending vibrations. In case of placebo microspheres, bands that appeared in both PEO-*g*-AAm and CS have also appeared in addition to a band at 1671 $cm^{-1}$, which indicates the formation of imine group. This confirms the crosslinking reaction between amine group of CS and aldehydic group of GA. The crosslinked structure is represented in Fig. 3.

FTIR spectral data were also used to confirm the chemical stability of capecitabine in the semi-IPN microspheres. For instance, FTIR spectra of: (a) pristine capecitabine, (b) placebo microspheres and (c) capecitabine-loaded microspheres are displayed in Fig. 10. Pristine capecitabine showed characteristic bands due to different functional groups. However, bands appearing at 3432 and 3234 $cm^{-1}$ are due to O–H/N–H stretching vibrations. The band at 1684 $cm^{-1}$ is due to pyrimidine carbonyl stretching vibrations, whereas bands at 1721 and 1756 $cm^{-1}$ are due to urethane carbonyl stretching vibrations. Characteristic bands at 1042 and 1202 $cm^{-1}$ indicate C–F stretching vibrations as well as the presence of tetrahydrofuran ring, respectively. When capecitabine is incorporated into semi-IPN microspheres, along with all other characteristic bands of placebo microspheres, some additional bands have appeared due to the presence of capecitabine in the matrix. However, some bands of capecitabine are not prominent in the drug-loaded microspheres due to merging of bands observed at frequencies 3234 and 1684 $cm^{-1}$ of the placebo microspheres as well as that of capecitabine at the same wave numbers. The characteristic bands of capecitabine observed at 1042, 1202 and 1721 $cm^{-1}$ have also appeared in the drug-loaded matrix without any change, which further indicates the chemical stability of drug in the semi-IPN matrix.

FTIR spectra of the pristine capecitabine and GA-treated capecitabine were compared (not displayed in Figs. 8–10) to investigate the possible reactions between them. It was observed that FTIR spectrum of GA-treated capecitabine was identical to that of the pristine capecitabine. In addition, a new peak observed at 1733 $cm^{-1}$ is due to the presence of the unreacted GA, which further confirms the chemical stability of capecitabine in the presence of GA.

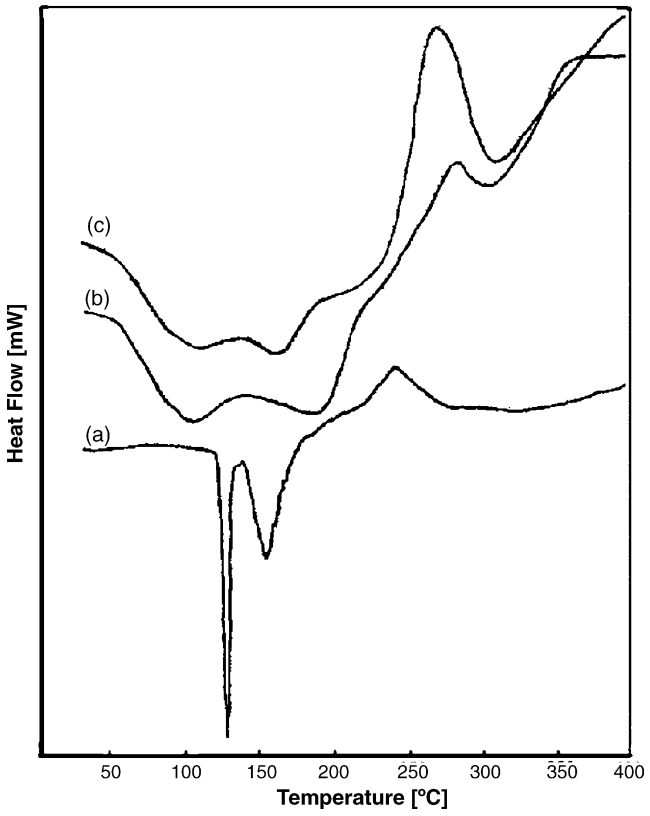


Fig. 11. DSC thermograms of: (a) pristine capecitabine, (b) capecitabine-loaded microspheres (formulation F2) and (c) placebo microspheres of formulation F2.

### 3.5. DSC studies

DSC thermograms of: (a) pristine capecitabine, (b) capecitabine-loaded microspheres and (c) placebo microspheres are presented in Fig. 11. In case of pristine capecitabine, two endothermic peaks were observed, one at 122 °C, which corresponds to melting process and the other at 150 °C due to thermal decomposition. Thermograms of placebo microspheres showed endothermic peaks at 107, 185 and 307 °C. Similarly, drug-loaded microspheres have shown the same pattern as that of placebo, but no peaks were observed at 122 and 150 °C, indicating the amorphous dispersion of drug into microspheres.

### 3.6. XRD studies

The X-ray diffraction spectra recorded for (a) pristine capecitabine, (b) capecitabine-loaded microspheres and (c) placebo microspheres are presented in Fig. 12. These results are useful to investigate the crystallinity of capecitabine in the crosslinked microspheres. Capecitabine has shown characteristic intense peaks at $2\theta$ of 5°, 20° and 25°, but in case of both the drug-loaded microspheres and placebo microspheres, no intense peaks were observed at $2\theta$ of 5°, 20° and 25°. Also, diffractograms of both the drug-loaded microspheres and placebo microspheres are almost identical, indicating the amorphous dispersion of drug after entrapment into polymeric microspheres.

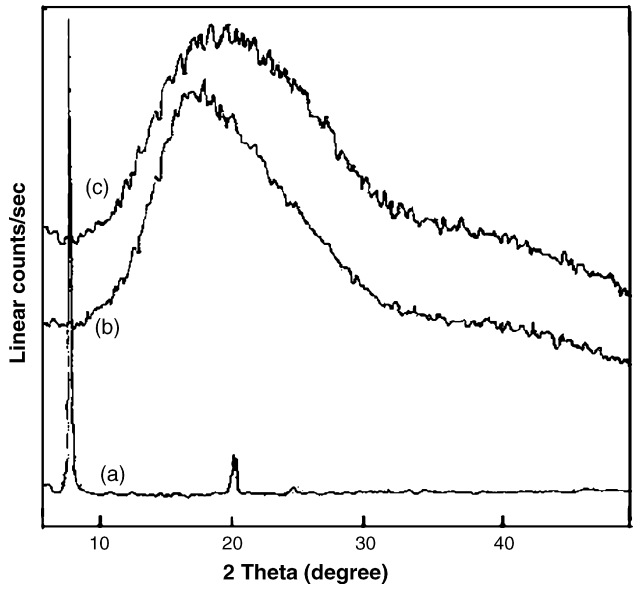


Fig. 12. XRD diffractograms of: (a) pristine capecitabine, (b) capecitabine-loaded microspheres (formulation F2) and (c) placebo microspheres of formulation F2.

### 3.7. Liquid transport/diffusion studies

Dynamic swelling experiments were performed gravimetrically in SIF media. These data are displayed in Fig. 13 for some typically chosen formulations, viz., F2, F6, F10 and F15. It was observed that swelling capacity of the microspheres decreased with an increasing amount of GA, due to the formation of a highly crosslinked rigid network. However, the swelling capacity of microspheres decreased with increasing amount of graft copolymer in the matrix due to the formation of a rigid semi-IPN structure as a result of entanglement of both polymeric chains. Decreased swelling of the microspheres at higher ratio of the graft copolymer can be explained as a result of decrease in the amount of chitosan of the network. Indeed, the polyelectrolyte nature of chitosan induces a high osmotic pressure and thus, a

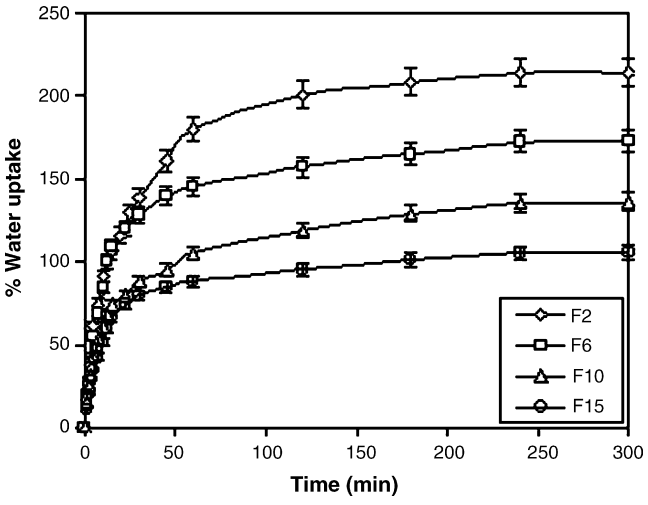


Fig. 13. Effect of extent of crosslinking on percentage of water uptake by the microspheres.

high swelling occurs due to increase in the translational entropy of counterions.

From the dynamic swelling results, it is possible to model the transport process to compute the diffusion coefficient, $D$. Diffusion occurs as a result of immersion of microspheres into the medium of interest and thereby, provoking absorption of the liquid by the polymer. Mathematical models are available (Vergnaud, 1991; Crank, 1975) to describe the sorption and desorption processes under simulated test conditions. Diffusion in spherically shaped matrices can be described by using Laplace transformation of the Fick's equation to calculate the mass uptake by the microspheres using:

$$\frac{M_t}{M_\infty} = 6\sqrt{\frac{Dt}{\pi^2}}\left(\frac{1}{\sqrt{\pi}} + 2\sum_{n=1}^{\infty}\text{ierf}\frac{nr}{\sqrt{Dt}}\right) - 3\frac{Dt}{r^2} \quad (6)$$

where $M_t$ is the amount of liquid released at time, $t$ and $M_\infty$ is total amount of liquid in the microsphere. Eq. (6) is quite complicated to solve. Baker and Lonsdale (1974) have derived a simple equation appropriate for the present case, after using the following initial and boundary conditions:

$$\text{Initial}: \quad t = 0, \quad r < R, \quad C = C_{\text{in}}$$

(inner part of microspheres)

$$\text{Boundary}: \quad t > 0, \quad r = R, \quad C = C_{\text{eq}}$$

(surface of microspheres)

In the above equations, $r$ is the initial radius, $R$ the radius of the swollen microsphere, and $C_{\text{in}}$ and $C_{\text{eq}}$ are, respectively concentrations at the beginning and at the end of the diffusion process. Diffusion coefficient can then be calculated for water absorption or drug release through microspheres by using:

$$D = \left(\frac{r\theta}{6M_\infty}\right)^2 \pi \quad (7)$$

where $\theta$ is slope of the linear portion of the plot of $M_t/M_\infty$ versus $t^{1/2}$ curves, $r$ initial radius of the microspheres, and $M_\infty$ is maximum equilibrium swelling value. The values of $D$ calculated in SIF media are included in Table 3. Diffusion coefficients fall in the range $(1.1–9.1) \times 10^{-6}\,\text{cm}^2\,\text{s}^{-1}$ and decrease systematically with increasing amount of the crosslinking agent as well as with increasing amount of graft copolymer composition of the microspheres. This may be attributed to the fact that with increasing amount of crosslinking agent, a stiffer semi-IPN matrix is likely to be formed, which would prohibit the transport of water molecules. Also, with increasing amount of graft copolymer in the matrix, the rate of swelling of microspheres decreased due to increased entanglement of CS and PEO-*g*-pAAm chains. This can also be explained by a decrease in the amount of chitosan of the network. Indeed, the polyelectrolyte nature of chitosan induces high osmotic pressure and thus high swelling to increase the translational entropy of the counterions.

### 3.8. Network parameters

Release of active agents from the polymer matrix depends upon the extent of crosslinking. Equilibrium swelling data were thus used to evaluate the network parameters of hydrogels. The two important structural parameters, viz., molar mass between crosslinks ($M_c$) and crosslink density ($d_x$) are considered in this work, since these are widely studied (Flory, 1953). When the hydrogel matrix is placed in a solvent, it would swell until elastic forces due to stretching of polymer chain segments balance the osmotic forces that could dissolve the polymer. Such elastic retractive forces are inversely proportional to molar mass of the polymer between crosslinks. Thus, lesser molar mass between two junction points results in a network structure that will be rigid and exhibits a limited swelling. When $M_c$ is large, the network is more elastic and swells rapidly when in contact with the compatible liquid. In the present case, it is an average molar mass between entanglements in the semi-IPN structure.

In order to assess the $M_c$ values, Flory–Rehner equation (Flory, 1953) in the following form was used:

$$M_c = -\rho_p V_s \phi^{1/3}[\ln(1-\phi) + \phi + \chi\phi^2]^{-1} \quad (8)$$

The volume fraction, $\phi$ of the polymer in the swollen state was calculated as:

$$\phi = \left[1 + \frac{\rho_p}{\rho_s}\left(\frac{M_a}{M_b}\right) - \frac{\rho_p}{\rho_s}\right]^{-1} \quad (9)$$

In the above equations, $\rho_p$ and $\rho_s$ are the densities of polymer (calculated by benzene displacement method) and solvent (calculated by densitymeter), respectively; $M_b$ and $M_a$ are, respectively, the mass of polymer before and after swelling and $V_s$ is the molar volume of the solvent ($18\,\text{cm}^3/\text{mol}$). Interaction parameter, $\chi$ was calculated using the equation proposed by Bristow and Watson (1958):

$$\chi = \beta + \left(\frac{V_s}{RT}\right)(\delta_s - \delta_p)^2 \quad (10)$$

Here $\beta$ is a lattice constant, whose value is taken to be 0.34, $V_s$ the molar volume of the solvent, $R$ the molar gas constant and $T$ is the temperature in K (310.15 K). The symbols $\delta_s$ and $\delta_p$ are solubility parameters of solvent and polymer, respectively. The value of $\delta_s$ was taken as $49.7\,\text{MPa}^{1/2}$ and $\delta_p$ was calculated by the group contribution method (Rudin, 1998).

The crosslink density ($d_x$) was calculated as (Savas and Guven, 2001):

$$d_x = \frac{1}{vM_c} \quad (11)$$

Here $v$ is the specific volume of the polymer. The results of $M_c$ (g/mol) and $d_x$ (mol/cm$^3$) are presented in Table 3. The $M_c$ values varied in the range from 1682 to 6758, while $d_x$ values are in the range between $3.21 \times 10^{-4}$ and $13.16 \times 10^{-4}$. These data indicate that $M_c$ values decrease with increasing amount of GA in the formulation, since the network would become denser. Also, $M_c$ values decreased with increasing graft copolymer composition of the formulation, indicating the formation of a dense struc-

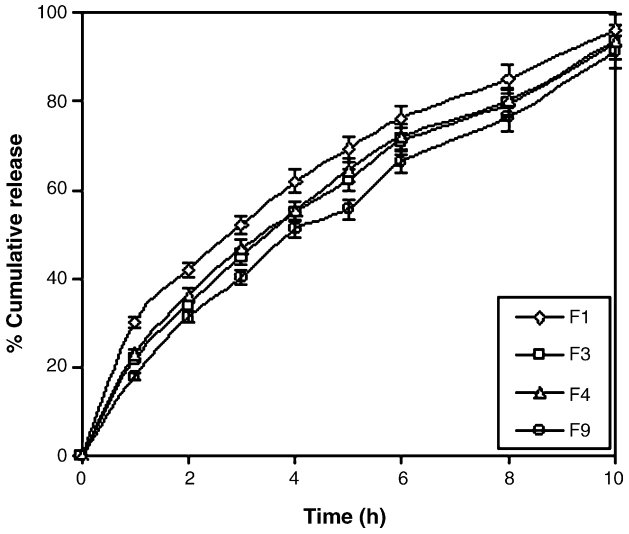


Fig. 14. Effect of extent of crosslinking on *in vitro* release profiles.

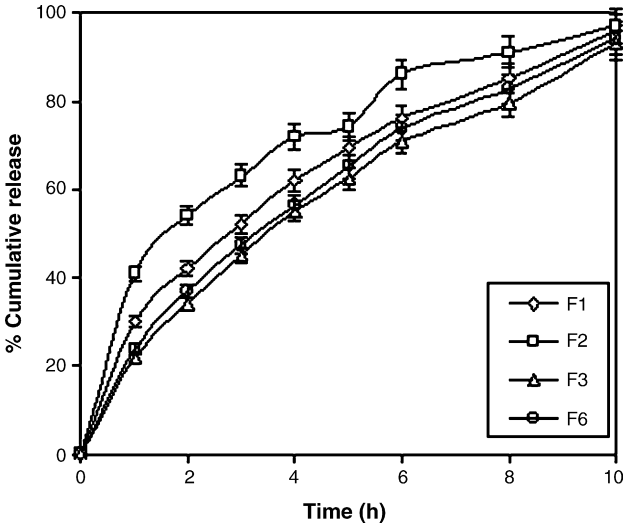


Fig. 15. Effect of percentage of drug loading on *in vitro* release profiles.

ture. Similarly, an amount of GA used and the graft copolymer contents in the formulations significantly affected the crosslink density of the semi-IPNs.

### 3.9. In vitro drug release

*In vitro* drug release studies were performed in SGF followed by SIF media (without enzymes). The dependence of the extent of crosslinking on *in vitro* release is displayed in Fig. 14, typically for four formulations, viz., F1, F3, F4 and F9. It is observed that release rates depend upon the amount of GA used during crosslinking. Release was slower for formulations in which higher amount of GA was used as compared to those formulations in which lower amount of GA was present in the matrix. This could be due to the fact that at higher crosslinking, free volume of the matrix will decrease, thereby hindering the transport of drug molecules through the matrix. This could also reduce the rate of swelling as well as the rate of drug release from the matrix. In Fig. 14, it can be seen that for formulation F1, the release is faster as compared to formulation F3, which contains a higher amount of GA. Similar trend is observed between formulations F4 and F9. The release rate can be correlated with the diffusion coefficient (see Table 3), which indicates that as the diffusion coefficient increases, the release rate also has increased.

To study the effect of percentage of drug loading on drug release rates, we have chosen four formulations, viz., F1, F2, F3 and F6. These results are displayed in Fig. 15. The release rates are slower for formulations containing lower amount of drug, while the release rate increased with increasing amount of drug in the microspheres. The drug in the polymer matrix might be acting as inert filler by occupying the free volume spaces of the swollen hydrogel. Capecitabine within the semi-IPN matrix acts as plasticizer and thus, increases the free volume within the network. This in turn, will create a more tortuous path for water molecules to permeate through, but the degree of tortuosity depends upon the volume fraction of the filler (Peppas, 1980). From Fig. 15, it can be seen that for formulation F2, the release is faster when compared to formulation F1, which contains lower amount of drug. Similar trends are observed between formulations F6 and F3.

The percentage of cumulative release versus time curves for microspheres prepared by using different ratios of graft copolymer:chitosan matrices are presented in Fig. 16 for formulations F8, F14, F10 and F15. Drug release rates are higher for microspheres having lower amount of graft copolymer compared to those having higher amount of graft copolymer. This further explains the formation of stiffer polymeric chain entanglements at higher amount of graft copolymer in the semi-IPN, thus reducing the rate of swelling as well as release of the drug. From Fig. 16, one can visualize that drug release is faster for formulation F8 as compared to F14, which contains higher amount of the graft copolymer. Similar trends can be seen between formulations F10 and F15. Drug release rate was also affected by the grafting ratio, i.e., composition of the copolymer. The release rates for formulations F12, F16, F1 and F5 are compared in

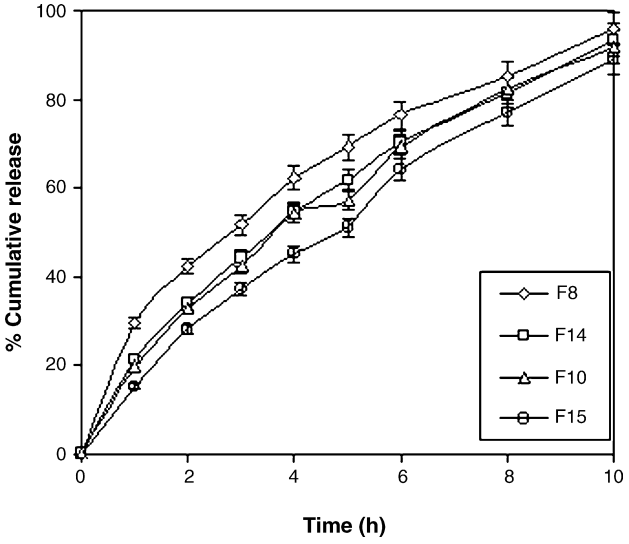


Fig. 16. Effect of graft copolymer:chitosan ratios on *in vitro* release profiles.

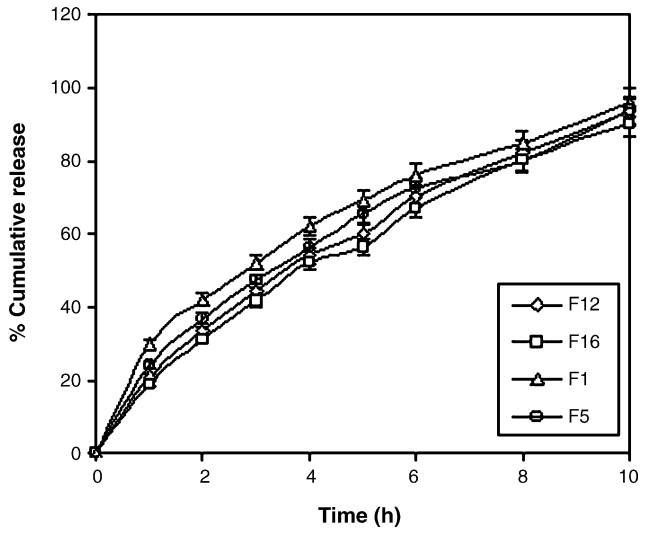


Fig. 17. Effect of grafting ratio on *in vitro* release profiles.

Fig. 17, wherein it was seen that capecitabine release from the microspheres was slightly faster in case of formulations with lower grafting ratio, i.e., polymer:monomer ratio of 1:5 as compared to formulations having the grafting ratio of 1:10 in the matrix. This could be due to increased entanglements of the semi-IPN chains due to the large number of side chains at higher grafting ratio. Experimental data displayed in Figs. 13–17 are in good agreement with the theoretical predictions made in the factorial design experiments.

Release results were also analyzed using the empirical equation (Ritger and Peppas, 1987). The initial 60% drug release data (i.e., linear region of the plots) were fitted to Eq. (12) to estimate the release kinetic parameter, $k$ and the diffusional exponent, $n$:

$$\frac{M_t}{M_\infty} = kt^n \tag{12}$$

By applying the least-squares estimation method to the release data at 95% confidence level, the values of $k$ and $n$ have been determined. These data along with the values of correlation coefficient, $r$ are presented in Table 3. Values of $k$ decrease with increasing crosslink density as well as with increasing ratio of the graft copolymer in the semi-IPN matrix. The $k$-values are small and range between 0.018 and 0.062, indicating mild-type of interactions between the drug and the polymer matrices. On the other hand, values of $n$ increased with increasing crosslink density as well as with increasing ratio of the graft copolymer in the semi-IPN matrix. These values ranged between 0.69 and 0.97, suggesting that the drug release mechanism can vary from anomalous to Case II transport (Baker and Lonsdale, 1974), depending upon the variation in the composition of formulations.

The novel material synthesized in the present research, PEO-*g*-pAAm is found to form a potential hydrogel, which can find applications in the CR of capecitabine. The material has a good controlled swelling/release behavior and found to hold the encapsulated drug for a longer period of time (longer drug retaining capacity). The PEO-*g*-pAAm utilizes the properties of all the three most widely used hydrogel polymers, viz., chitosan, PEO and pAAm. It can thus be regarded as material of choice for CR formulation of other water-soluble drugs.

## 4. Conclusions

Semi-interpenetrating network microspheres of chitosan with poly(ethylene oxide)-*g*-polyacrylamide were prepared by emulsion crosslinking method. Capecitabine, an anticancer drug, was successfully encapsulated into semi-IPN matrix with percentage of encapsulation efficiency ranging between 79 and 87. Microspheres formed were spherical in nature with smooth surfaces having particle size in the range of 82–168 μm. The results of $2^4$ factorial design experiment indicated a significant contribution of all the four main effects of grafting ratio, ratio of graft copolymer:chitosan, amount of GA used and percentage of drug loading on percentage of drug release at 5 h (response). Crosslink density of the prepared matrices was significantly affected by the amount of GA used and the amount of graft copolymer used to prepare the formulations. The release of capecitabine depends upon the extent of crosslinking, percentage of drug loading, amount of graft copolymer used in the matrix as well as grafting ratio of the polymer. Higher release rates were observed for microspheres with lower crosslink density and lower amount of graft copolymer in the matrix. The drug release mechanisms vary from anomalous to Case II transport, depending upon the formulation variables. In conclusion, this work demonstrates the feasibility of preparing semi-IPN hydrogel matrices by physical blending of the biocompatible polymers such as chitosan and poly(ethylene oxide)-*grafted*-polyacrylamide that are crosslinked with GA.

## Acknowledgements

The authors appreciate the financial support from University Grants Commission (UGC), New Delhi, India (F1-41/2001/CPP-II) in establishing Center of Excellence in Polymer Science. They also thank Professor I.D. Shetty, Department of Statistics, Karnatak University for useful discussions on the statistical analyses.

## References

Agnihotri, S.A., Aminabhavi, T.M., 2004a. Formulation and evaluation of novel tableted chitosan microparticles for the controlled release of clozapine. J. Microencapsul. 21, 709–718.

Agnihotri, S.A., Aminabhavi, T.M., 2004b. Controlled release of clozapine through chitosan microparticles prepared by a novel method. J. Control. Release 96, 245–259.

Agnihotri, S.A., Mallikarjuna, N.N., Aminabhavi, T.M., 2004. Recent advances on chitosan-based micro and nanoparticles in drug delivery. J. Control. Release 100, 5–28.

Agnihotri, S.A., Aminabhavi, T.M., 2005. Development of novel interpenetrating network gellan gum-poly(vinyl alcohol) hydrogel microspheres for the controlled release of carvedilol. Drug Dev. Ind. Pharm. 31, 491–503.

Akbuga, J., Durmaz, G., 1994. Preparation and evaluation of cross-linked chitosan microspheres containing furosemide. Int. J. Pharm. 111, 217–222.

Apicella, A., Cappello, B., Del Nobile, M.A., La Rotonda, M.I., Mensitieri, G., Nicolais, L., 1993. Poly(ethylene oxide) (PEO) and different molecular weight PEO blends monolithic devices for drug release. Biomaterials 14, 83–90.

Baker, R.W., Lonsdale, H.K., 1974. Controlled release: mechanisms and rates. In: Tanquarry, A.C., Lacey, R.E. (Eds.), Controlled Release of Biologically Active Agents. Plenum Press, New York, pp. 15–71.

Bristow, G.M., Watson, W.F., 1958. Cohesive energy density of polymers. I. Cohesive energy densities of rubbers by swelling measurements. Trans. Faraday Soc. 54, 1731–1741.

Calvo, P., Remunan-Lopez, C., Vila-Jata, J.L., Alonso, M.J., 1997. Novel hydrophilic chitosan-polyethylene oxide nanoparticles as protein carriers. J. Appl. Polym. Sci. 63, 125–132.

Changez, M., Burugapalli, K., Koul, V., Choudhary, V., 2003. The effect of composition of poly (acrylic acid)-gelatin hydrogel on gentamicin sulphate release *in vitro*. Biomaterials 24, 527–536.

Crank, J., 1975. The Mathematics of Diffusion, 2nd ed. Clarendon, Oxford.

Daniel, W.W., 1987. Biostatistics: A Foundation for Analysis in the Health Sciences, 5th ed. Wiley, New York.

Doelker, E., 1987. Water-swollen cellulose derivatives in pharmacy. In: Peppas, N.A. (Ed.), Hydrogels in Medicine II. CRC Press, Boca Raton, FL, p. 115.

Ekici, S., Saraydin, D., 2004. Synthesis, characterization and evaluation of IPN hydrogels for antibiotic release. Drug Deliv. 11, 381–388.

Flory, P.J., 1953. Principles of Polymer Chemistry. Cornell University, Ithaca, New York.

Judson, I.R., Beale, P.J., Trigo, J.M., Aherne, W., Crompton, T., Jones, D., Bush, E., Reigner, B., 1999. A human capecitabine excretion balance and pharmacokinetic study after administration of a single oral dose of $^{14}$C-labelled drug. Invest. New Drugs 17, 49–56.

Kosmala, J.D., Henthorn, D.B., Peppas, L.B., 2000. Preparation of interpenetrating networks of gelatin and dextran as degradable biomaterials. Biomaterials 21, 2019–2023.

Kulkarni, A.R., Soppimath, K.S., Aminabhavi, T.M., Rudzinski, W.E., 2001. *In vitro* release kinetics of cefadroxil-loaded sodium alginate interpenetrating network beads. Eur. J. Pharm. Biopharm. 51, 127–133.

Kurkuri, M.D., Aminabhavi, T.M., 2004. Poly(vinyl alcohol) and poly(acrylic acid) sequential interpenetrating network pH sensitive microspheres for the delivary of diclofenac sodium to the intestine. J. Control. Release 96, 9–20.

Mi, F.L., Shyu, S.S., Chen, C.T., Schoung, J.Y., 1999. Porous chitosan microspheres for controlling the antigen release of Newcastle disease vaccine: preparation of antigen-adsorbed microsphere and *in vitro* release. Biomaterials 20, 1603–1612.

Montgomery, D.C., 1997. Design and Analysis of Experiments, 4th ed. Wiley, New York, pp. 290–341.

Peppas, N.A., 1980. Mathematical modeling of diffusion process in drug delivery polymeric systems. In: Smolen, V.F. (Ed.), Bioavailability and the Pharmacokinetic Control of Drug Response. Wiley, New York.

Ravi Kumar, M.N.V., 2001. A review of chitin and chitosan applications. React. Funct. Polym. 46, 1–27.

Razaghi, A.M., Schwartz, J.B., 2002. Investigation of cyclobenzaprine hydrochloride release from oral osmotic delivery systems containing a water swellable polymer. Drug Dev. Ind. Pharm. 28, 631–639.

Risbud, M.V., Bhonde, R.R., 2000. Polyacrylamide-chitosan hydrogels: *in vitro* biocompatibility and sustained antibiotic release studies. Drug Deliv. 7, 69–75.

Ritger, P.L., Peppas, N.A., 1987. A simple equation for description of solute release. II. Fickian and anomalous release from swellable devices. J. Control. Release 5, 37–42.

Rudin, A., 1998. The Elements of Polymer Science and Engineering, 2nd ed. Academic Press, San Diego, CA, pp. 445–483.

Savas, H., Guven, O., 2001. Investigation of active substance release from poly(ethylene oxide) hydrogels. Int. J. Pharm. 224, 151–158.

Sperling, L.H., 1981. Interpenetrating Polymer Networks and Related Materials. Plenum Press, New York, p. 1.

Soppimath, K.S., Kulkarni, A.R., Aminabhavi, T.M., 2000. Controlled release of antihypertensive drug from the interpenetrating network poly(vinyl alcohol)-guar gum hydrogel microspheres. J. Biomater. Sci. Polym. Ed. 11, 27–43.

Verestiuc, L., Ivanov, C., Barbu, E., Tsibouklis, J., 2004. Dual-stimuli-responsive hydrogels based on poly(*N*-isopropylacrylamide)/chitosan semi-interpenetrating networks. Int. J. Pharm. 269, 185–194.

Vergnaud, J.M., 1991. Liquid Transport Processes in Polymeric Materials—Modeling and Industrial Applications. Prentice Hall, Englewood Cliffs, NJ.

Zhang, F., McGinity, J.W., 1999. Properties of sustained-release tablets prepared by hot-melt extrusion. Pharm. Develop. Technol. 4, 241–250.